

Photometry of neglected open clusters in the First and Fourth Galactic Quadrants

Giovanni Carraro^{1,2}, ^{*} Kenneth A. Janes³ and Jason D. Eastman^{3,4} [†]

¹*Departamento de Astronomía, Universidad de Chile, Casilla 36-D, Santiago, Chile*

²*Astronomy Department, Yale University, P.O. Box 208101, New Haven, CT 06520-8101, USA*

³*Department of Astronomy, Boston University, 725 Commonwealth Avenue, Boston, MA 02215, USA*

⁴*Department of Astronomy, Ohio State University, 140 West 18th Avenue, Columbus, OH 43210, USA*

Submitted: July 2005

ABSTRACT

CCD *BVI* photometry is presented for 8 previously unstudied star clusters located in the First and Fourth Galactic Quadrants: AL 1, BH 150, NGC 5764, Lynga 9, Czernik 37, BH 261, Berkeley 80 and King 25. Color magnitude diagrams of the cluster regions suggest that several of them (BH 150, Lynga 9, Czernik 37 and BH 261 and King 25) are so embedded in the dense stellar population toward the galactic center that their properties, or even their existence as physical systems, cannot be confirmed. Lynga 9, BH 261 and King 25 appear to be slight enhancements of dense star fields, BH 150 is probably just a single bright star in a dense field, and Czernik 37 may be a sparse, but real cluster superimposed on the galactic bulge population. We derive preliminary estimates of the physical parameters for the remaining clusters. AL 1 appears to be an intermediate age cluster beyond the solar circle on the far side of the galaxy and the final two clusters, NGC 5764 and Berkeley 80 are also of intermediate age but located inside the solar ring. This set of clusters highlights the difficulties inherent in studying the stellar populations toward the inner regions of the galaxy.

Key words: Open clusters and associations: general – open clusters and associations: individual: AL 1, BH 150, NGC 5764, Lynga 9, Czernik 37, BH 261, Berkeley 80, King 25.

1 INTRODUCTION

According to the recent Galactic Open Clusters compilation by Dias et al. (2002, <http://www.astro.iag.usp.br/~wilton>), 1632 open clusters are known to exist in the Milky Way disk. Unfortunately, basic parameters like distance, reddening and age are available for fewer than half the clusters in this sample. This fact obviously limits the use of open clusters as probes of the structure and evolution of the Galactic disk. A large observational effort is clearly needed to improve on this situation.

This is particularly important for sparse, loose star clusters, which are hard to distinguish from the rich Galactic field and may be very close to the dissolution phase (Bonatto et al. 2004).

^{*} Andes Fellow, on leave from Dipartimento di Astronomia, Università di Padova, Vicolo Osservatorio 2, I-35122, Padova, Italy

[†] email: gcarraro@das.uchile.cl (GC), janes@bu.edu (KAJ), jdeast@bu.edu (JDE)

The statistics of open cluster ages are dramatically skewed towards young star clusters, which are both more numerous and often more visible (Wielen 1971). However in recent years new efforts have been done to provide observational material for intermediate-age and old star clusters (Phelps et al. 1994, Kaluzny 1994, Hasegawa et al. 2004, Carraro et al. 2005a, and references therein). All this new observational material will surely result in a revision of the open cluster age distribution and typical lifetime.

In this paper we present the first photometric study of 8 overlooked, faint and highly contaminated open clusters located in the Fourth and First Galactic Quadrant having $305^\circ \leq l \leq 49^\circ$ and $-5^\circ.2 \leq b \leq +5^\circ.9$ (see Table 1) and provide homogeneous derivation of basic parameters using the Padova (Girardi et al. 2000) family of isochrones.

The plan of the paper is as follows. Sect. 2 describes the observation strategy and reduction technique. Sect. 3 deals with the Color-Magnitude Diagrams (CMD) and illustrates

Table 1. Basic parameters of the clusters under investigation. Coordinates are for J2000.0 equinox and have been visually re-determined by us.

Name	<i>RA</i>	<i>DEC</i>	<i>l</i>	<i>b</i>
	<i>hh : mm : ss</i>	<i>° : ' : ''</i>	[deg]	[deg]
AL 1	13:15:16	-65:55:18	305.40	-3.20
BH 150	13:38:04	-63:20:45	308.11	-0.93
NGC 5764	14:53:33	-52:40:15	320.97	+5.86
Lynga 9	16:20:41	-48:32:00	334.51	+1.08
Czernik 37	17:53:14	-27:22:00	2.22	-0.63
BH 261	18:14:05	-28:38:00	3.35	-5.29
Berkeley 80	18:54:21	-01:13:00	32.17	-1.25
King 25	19:24:35	+13:42:14	48.86	-0.93

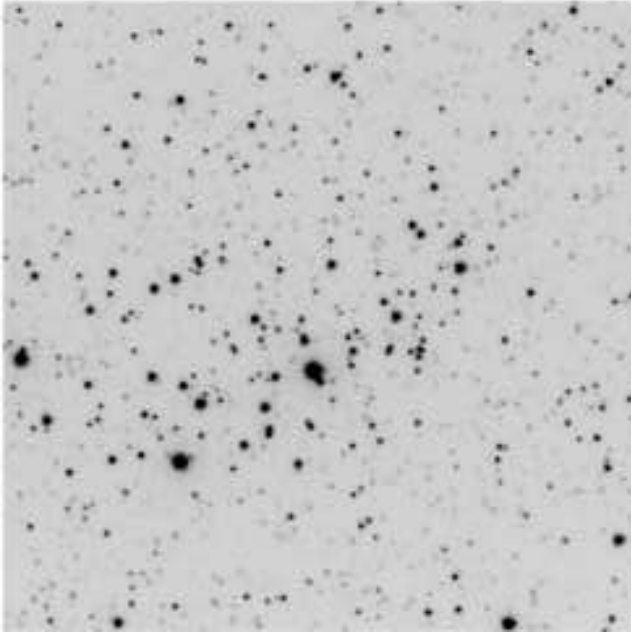


Figure 1. $I = 1200$ sec image of A-L 1. North is up, East on the left, and the covered area is $4'.1 \times 4'.1$.

the derivation of the clusters' fundamental parameters. Finally, Sect. 4 provides a detailed discussion of the results.

2 OBSERVATIONS AND DATA REDUCTION

CCD *BVI* observations were carried out with the CCD camera on-board the 1.0m telescope at Cerro Tololo Inter-american Observatory (CTIO, Chile), on the night of June 6, 2005. With a pixel size of $0''.469$, and a CCD size of 512×512 pixels, this samples a $4'.1 \times 4'.1$ field on the sky. The details of the observations are listed in Table 2 where the observed fields are reported together with the exposure times, the average seeing values and the range of air-masses during the observations. Figs. 1 to 8 show deep *I* images in the area of the clusters we observed.

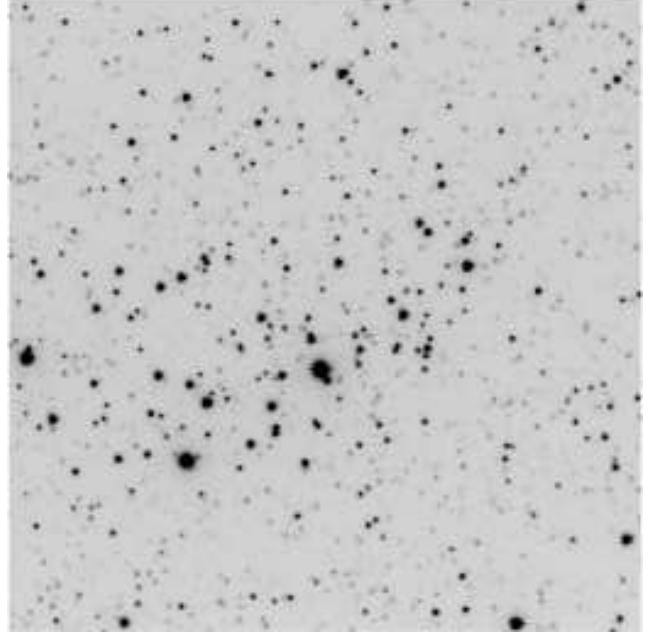


Figure 2. $I = 600$ sec image of Berkeley 80. North is up, East on the left, and the covered area is $4'.1 \times 4'.1$.

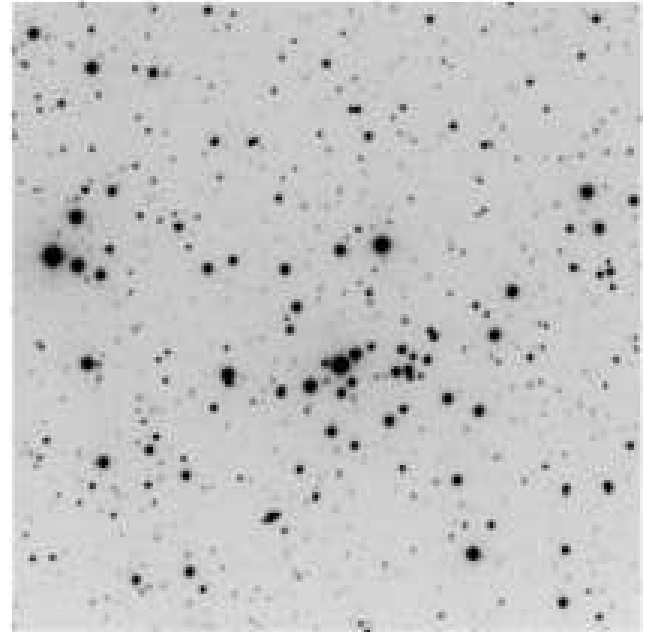


Figure 3. $I = 600$ sec image of NGC 5764. North is up, East on the left, and the covered area is $4'.1 \times 4'.1$.

The data have been reduced with the IRAF[‡] packages CCDRED, DAOPHOT, ALLSTAR and PHOTCAL using the point spread function (PSF) method (Stetson 1987). The night turned out to be photometric and very stable. We derived calibration equations for all the 80 standard stars observed during the night in the Landolt (1992)

[‡] IRAF is distributed by NOAO, which are operated by AURA under cooperative agreement with the NSF.

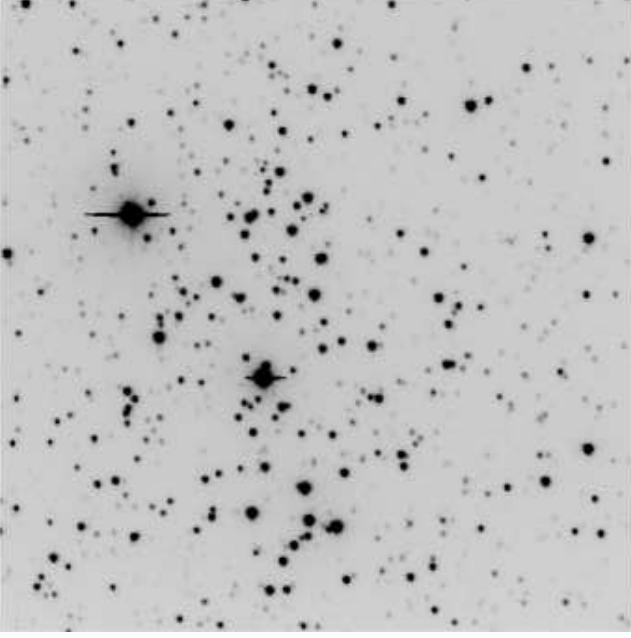


Figure 4. I = 600 sec image of Czernik 37. North is up, East on the left, and the covered area is $4'.1 \times 4'.1$.

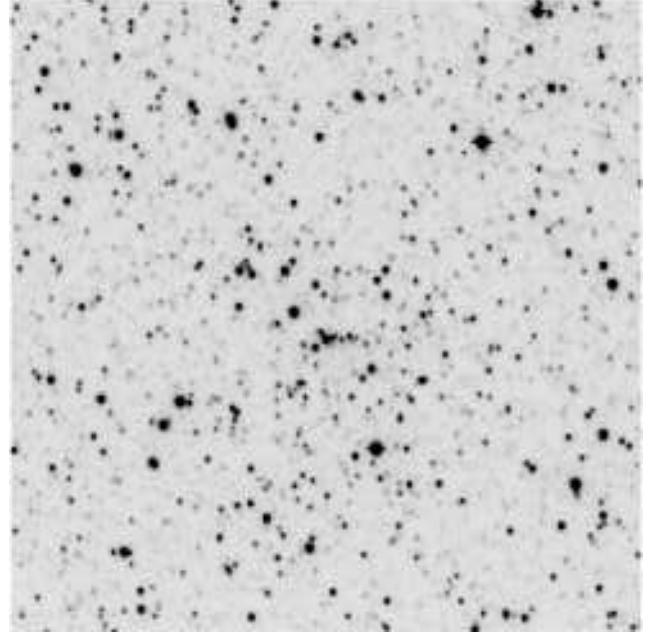


Figure 6. I = 600 sec image of BH 261. North is up, East on the left, and the covered area is $4'.1 \times 4'.1$.

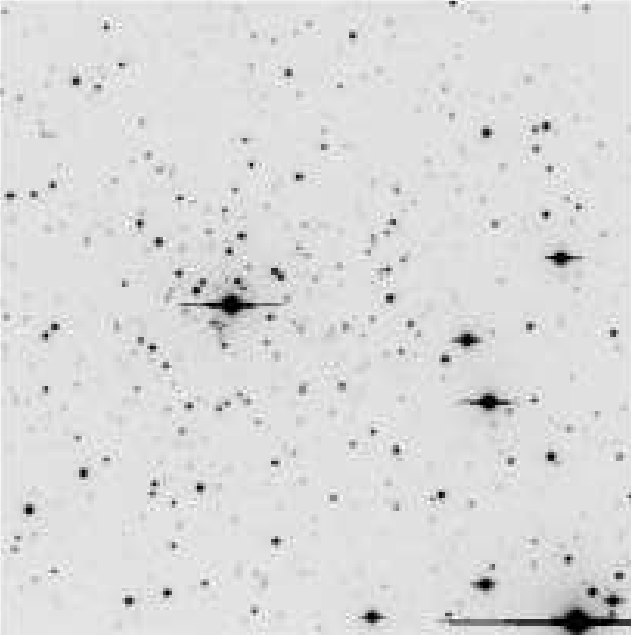


Figure 5. I = 600 sec image of BH 150. North is up, East on the left, and the covered area is $4'.1 \times 4'.1$.



Figure 7. B = 900 sec image of Lynga 9. North is up, East on the left, and the covered area is $4'.1 \times 4'.1$.

fields PG 1047+003, MarkA, PG 1323-085, PG 1633+099, PG 1657+078 and PG 2213-006 (see Table 2 for details). Together with the clusters, we observed two control fields 20 arcmins South of King 25, at 19:24:34.9, +13:22:15.3 (J2000.0), and 10 arcmins North of Lynga 9, at 16:20:40.8, -48:21:45.1 (J2000.0), to deal with field star contamination. In fact these are the only two clusters which extend beyond the field covered by the CCD. Exposure of 600 secs in V and I were secured for these fields.

The calibration equations are of the form:

$$\begin{aligned} b &= B + b_1 + b_2 \times X + b_3 (B - V) \\ v &= V + v_1 + v_2 \times X + v_3 (B - V) \\ v &= V + v_{1,i} + v_{2,i} \times X + v_{3,i} \times (V - I) \\ i &= I + i_1 + i_2 \times X + i_3 (V - I) , \end{aligned}$$

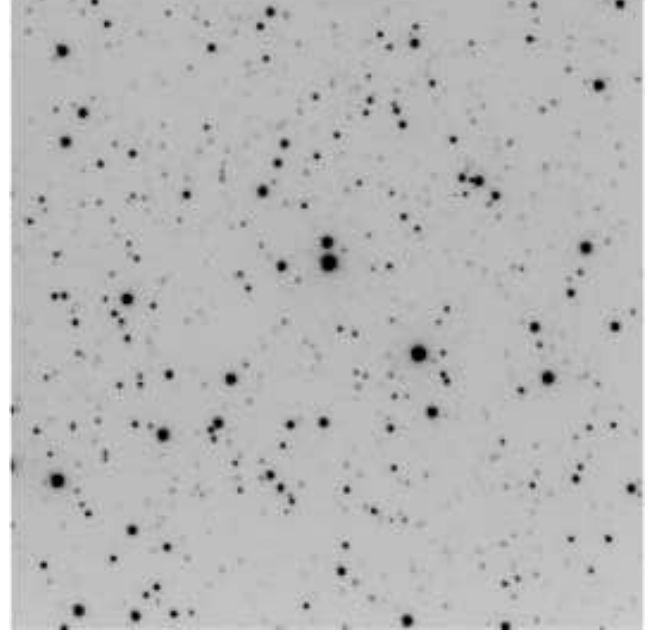
where BVI are standard magnitudes, bvi are the instrumental ones and X is the airmass; all the coefficient values are reported in Table 3. The standard stars in these fields pro-

Table 2. Journal of observations of clusters and standard star fields (June 6, 2005).

Field	Filter	Exposure time [sec.]	Seeing [\prime]	Airmass
AL 1	B	120,1200,1800	1.0	1.24
	V	30,600,1200	1.0	1.24
	I	30,600,1200	1.0	1.25
BH 150	B	120,1200	0.9	1.20
	V	30,600	0.8	1.20
	I	30,600	0.8	1.21
NGC 5764	B	120,1200	0.9	1.09
	V	30,600	1.0	1.09
	I	30,600	1.0	1.10
Lynga 9	B	120,900	1.0	1.07
	V	30,600	1.0	1.06
	I	30,600	0.8	1.05
Czernik 37	B	120,900	1.1	1.00
	V	30,600	1.0	1.00
	I	30,600	1.0	1.01
BH 261	B	120,900	1.0	1.01
	V	30,600	0.9	1.01
	I	30,600	0.9	1.02
Berkeley 80	B	120,900	0.8	1.16
	V	30,600	0.8	1.19
	I	30,600	0.8	1.21
King 25	B	120,1200	1.0	1.43
	V	30,600	1.0	1.49
	I	30,600	1.0	1.52
MarkA	B	2 \times 120	1.0	1.24-1.46
	V	2 \times 40	1.0	1.24-1.46
	I	2 \times 20	1.1	1.24-1.46
PG 1323-085	B	3 \times 120	1.1	1.00-1.91
	V	3 \times 40	1.1	1.00-1.91
	I	3 \times 20	1.0	1.00-1.91
PG 1633+099	B	3 \times 120	1.1	1.20-1.74
	V	3 \times 40	1.1	1.20-1.74
	I	3 \times 20	1.0	1.20-1.74
PG 1657+078	B	4 \times 120	1.1	1.06-1.34
	V	4 \times 40	1.0	1.06-1.34
	I	4 \times 20	0.9	1.06-1.34
PG 2213-006	B	3 \times 120	1.1	1.00-1.54
	V	3 \times 40	1.0	1.00-1.54
	I	3 \times 20	1.0	1.00-1.54
PG 1047+003	B	3 \times 120	1.1	1.18-1.47
	V	3 \times 40	0.9	1.18-1.47
	I	3 \times 20	0.9	1.18-1.47

Table 3. Coefficients of the calibration equations

$b_1 = 3.573 \pm 0.009$	$b_2 = 0.25 \pm 0.02$	$b_3 = -0.155 \pm 0.008$
$v_1 = 3.447 \pm 0.005$	$v_2 = 0.16 \pm 0.02$	$v_3 = -0.019 \pm 0.005$
$v_{1,i} = 3.448 \pm 0.005$	$v_{2,i} = 0.16 \pm 0.02$	$v_{3,i} = -0.016 \pm 0.005$
$i_1 = 4.338 \pm 0.005$	$i_2 = 0.08 \pm 0.02$	$i_3 = -0.022 \pm 0.005$

**Figure 8.** I = 600 sec image of King 25. North is up, East on the left, and the covered area is $4'.1 \times 4'.1$.

vide a very good color coverage. The final global *r.m.s.* (calibration plus DAOPHOT internal errors) are 0.033, 0.031 and 0.031 for the B, V and I filters, respectively (Patat & Carraro 2001).

We generally used the third equation to calibrate the *V* magnitude in order to get the same magnitude depth both in the cluster and in the field. The limiting magnitudes are $B = 21.9$, $V = 22.5$ and $I = 21.8$. Moreover we performed a completeness analysis following the method described in Baume et al. (2005). It turns out that our sample has completeness level larger than 50% down to $B = 20.0$, $V = 21.0$ and $I = 20.5$.

The final photometric catalogs for (coordinates, B, V and I magnitudes and errors) consist of 3392, 1949, 1537, 1373, 1178, 3729, 1738 and 883 stars for AL 1, BH 150, NGC 5764, Lynga 9, Czernik 37, BH 261, Berkeley 80 and King 25, respectively, and are made available in electronic form at the WEBDA[§] site maintained by J.-C. Mermilliod.

3 COLOUR-MAGNITUDE DIAGRAMS AND CLUSTER PARAMETERS

In this section we describe cluster CMDs and derive their basic parameters.

We first evaluated the CMD data as well as images from the 2-Micron All Sky Survey (2MASS) all sky data release (available at www.ipac.caltech.edu/2mass/releases/allsky) to explore the existence of the clusters as physical systems. The 2MASS K_s images are substantially less affected by reddening than the visual images which means that in some cases, the confusion from background galactic stars can be

[§] <http://obswww.unige.ch/webda/navigation.html>

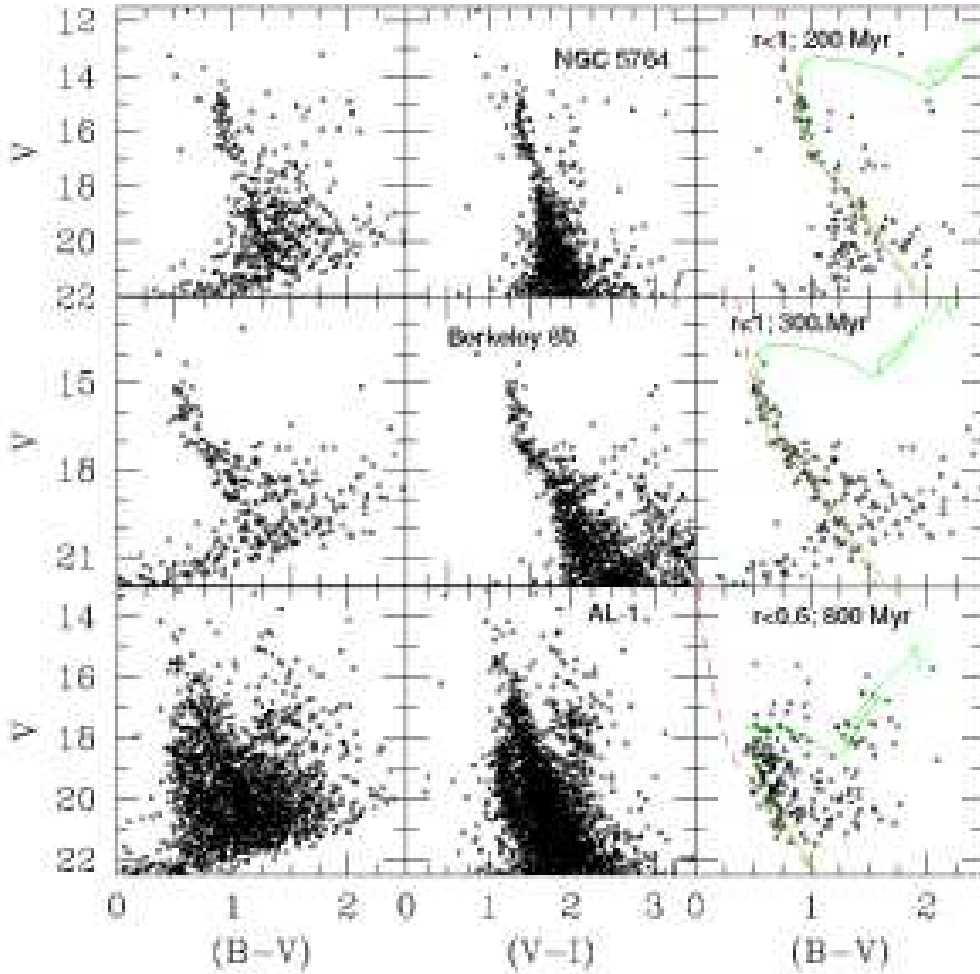


Figure 9. CMDs of the stars in the field of AL 1, Berkeley 80 and NGC 5764. **Left panels:** all the stars in the V vs $(B-V)$ diagrams. **Central panels:** all the stars in the V vs $(V-I)$ diagrams. **Right panels:** Stars lying within r arcmin from the cluster center (indicated for each cluster). The dashed line is the empirical ZAMS from Schmidt-Kaler (1982), whereas the solid lines are isochrones from Girardi et al. (2000) for the solar metallicity and the indicated age.

higher, but the background should often also be less variable.

Distance moduli, reddenings and ages of the confirmed clusters have been derived by matching the observed CMDs to isochrones from the Padova group (Girardi et al. 2000) by eye, paying particular attention to the shape of the MS, the position of the brightest MS stars, the turn-off point and the location of evolved stars, if present.

To infer the heliocentric distances we adopted $R_V = A_V/E(B-V) = 3.1$

The theoretical isochrones are available for a wide range of metallicities. We have adopted for all clusters those with a solar value because of a lack of firm photometric or spectroscopic determinations of metallicities of individual clusters. The effect of metallicity has been frequently considered in literature: increasing it shifts the isochrones fitting toward older ages, larger distances and smaller reddening.

The results are summarized in Table 4, where the basic parameters are listed together with their uncertainties. The

latter correspond to the shift allowed to isochrone fitting before a mismatch is clearly perceived by eye inspection.

3.1 AL 1

This cluster was discovered by Andrews & Lindsay (1967) and then independently by van den Bergh & Hagen (1975) who named it BH 144. It is described as a faint, moderately populated object, with a diameter of 1.5 arcmin, clearly visible both on red and on blue plates (see Fig. 1). The 2MASS K_s image also shows the cluster just at the limiting magnitude of the image. Its CMDs are shown in Fig. 9, lower panels. Both the left-hand side and central panel clearly show the presence of a strong contamination by the Galactic disk in a form resembling a Main Sequence (MS). The cluster lies on the left of the disk MS. The evolved region is also complicated by foreground contamination. However a selection in radius (0.6 arcmin) makes the cluster emerging. A

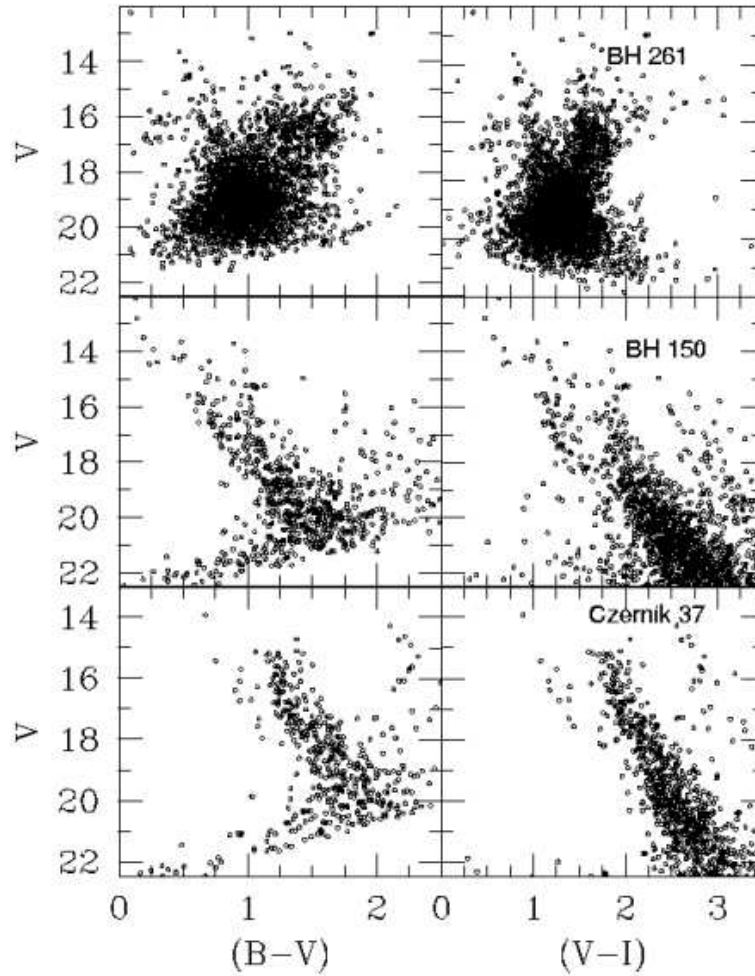


Figure 10. CMDs of the stars in the field of Czernik 39, BH 150 and NGC 261. **Left panels:** all the stars in the V vs $(B-V)$ diagrams. **Right panels:** all the stars in the V vs $(V-I)$ diagrams.

suggested match to an 800 Myr isochrone yields a reddening $E(B-V)=0.35$ and a distance modulus $(m-M) = 17.2$. This implies a distance from the Sun of 19.9 kpc.

3.2 Berkeley 80

This cluster was detected by Setteducati & Weaver (1960). Dias et al. (2002) report a diameter of 4 arcmin for Berkeley 80 (see also Fig. 2). A small group of stars is visible at this position on the 2MASS K_s image. Its CMDs are shown in Fig. 9, middle panels and resemble somewhat the CMD of NGC 5764 (see Fig. 9). A possible match to a 300 Myr isochrone suggests a reddening $E(B-V)=1.1$ and a distance modulus $(m-M) = 14.8$. This implies a distance from the Sun of 3.3 kpc.

3.3 NGC 5764

This cluster is also listed as BH 167 by van den Bergh & Hagen (1975) who described it as a very poorly populated object, with a diameter of 2.5 arcmin, visible only on blue plates. The cluster is also visible on our I-band image (see Fig 3) and the 2MASS K_s image. Its CMDs are shown in Fig. 9, upper panels. Because of its distance from the Galactic Plane, this cluster better emerges from the background, showing a clear MS from $V=14$ to $V=19$. The right-hand panel of Fig. 9 shows the central 1 arcmin region of the cluster region matched to a 200 Myr isochrone, yielding a reddening $E(B-V)=1.0$ and a distance modulus $(m-M) = 15.3$. This implies a distance from the Sun of 2.8 kpc

3.4 Czernik 37

Czernik (1966) described this as a cluster with diameter of 3 arcmin and fewer than 50 stars (see also Fig. 4). The cluster is also listed as BH 253 by van den Bergh & Hagen (1975), who described it as a moderately populated object with the

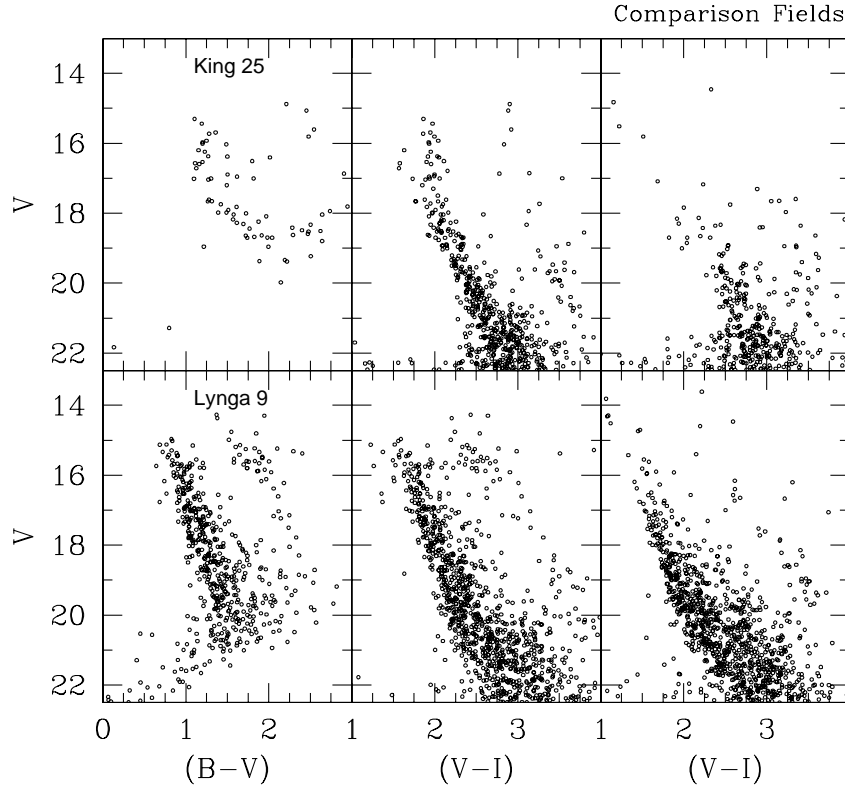


Figure 11. CMDs of the stars in the field of Lynga 9 and King 25 and their offset fields. **Left panels:** all the cluster stars in the V vs $(B-V)$ diagram. **Middle panels:** all the cluster stars in the V vs $(V-I)$ diagram. **Right panels:** all the field stars in the V vs $(V-I)$ diagram

same diameter. This cluster is projected onto the central bulge of the galaxy, only 2 degrees from the direction to the galactic center. The 2MASS image shows an extremely dense star field, with an asterism very much like the pattern visible in Fig. 4. Its CMDs are shown in Fig. 10, lower panels. Although there is an appearance of a broad main sequence in the CMD, it may just be an artifact of the increasing star density in this direction. The status of this possible cluster is rather uncertain.

3.5 BH 150

van den Bergh & Hagen (1975) described this cluster as a faint, poorly populated object, with a diameter of 2.5 arcmin, visible only on blue plates, but questionable in the red plate. In Fig. 5 and the 2MASS K_s image a bright star appears right at the cluster position, which may cause the impression of a small cluster. Its CMDs are shown in Fig. 10, middle panels. The CMDs for this region are dominated by the galactic plane population along this line of sight. The evidence for a cluster at this position is weak at best.

3.6 BH 261

This possible cluster was discovered by van den Bergh & Hagen (1975), who describe it as a moderately populated cluster having a diameter of 1.5 arcmin, clearly visible both on red and on blue plates. Fig. 6 shows no indication of a cluster, nor is there any sign of a cluster on the 2MASS K_s image. Its CMDs are shown in the upper panels of Fig. 10. The galactic contribution is very large and the field very rich. There probably is no cluster at this position.

3.7 Lynga 9

This asterism was first noted by Lynga (1964), and later by van den Bergh & Hagen (1975), who named it BH 189, and described it as a moderately populated cluster having a diameter of 6 arcmin, clearly visible both on red and on blue plates (see Fig. 7). The 2MASS images show no indication of a cluster. Its CMDs are shown in Fig. 11, together with a comparison field (upper right panel) taken 10 arcmin away from the cluster center (see Sect. 2).

Since we have the comparison field images for Lynga 9, it is possible to go into somewhat greater depth in our analysis of Lynga 9 than we can with the other clusters. Assuming that the overall distribution of stars in the field region is the same as the galactic background in the clus-

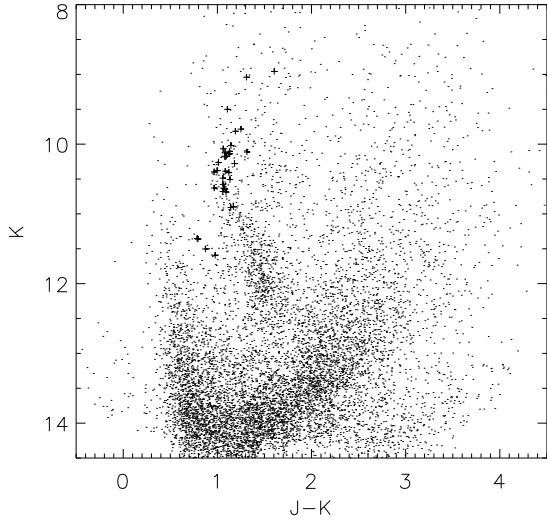


Figure 12. K vs J-K cmd for 2mass stars within a 10 arcminute field of view around the Lynga 9 position. The plus signs indicate the Lynga 9 "clump" stars from Fig. 11 with V between 14.5 - 16.5 and V-I between 2 - 3

ter field, it is possible to subtract possible field stars from the cluster region with the following simple procedure. For each star in the field region, we simply deleted whatever star in the cluster region is closest in color and magnitude to the target field star. If the general background of stars is the same in the field region and the cluster region, and if there really is a cluster, this process would leave an excess of stars in the cluster field, most of which would presumably be cluster stars.

In the case of Lynga 9, the star-subtraction process eliminates all stars in the cluster region except for a few stars at the top of the "main sequence" and a group of stars that resemble a red giant clump at $V=15.5$ and $V-I=2.5$. Fainter than about $V=16$, the field region and the cluster region are virtually identical. If the apparent "clump" stars really were red giants, there would have to be a corresponding well-populated main sequence in the cluster region. So there just cannot be an ordinary cluster there.

So what is that clump of stars? There certainly is the appearance of a sparse cluster on the red and blue sky survey images, but the 2MASS images show no indication of a cluster at all. However, a K,J-K color-magnitude diagram for a field with a 10-arcminute radius around the cluster shows a prominent population of stars near $K=12$ and $J-K=1.5$, together with a sequence of stars extending brighter and to the blue (Fig. 12).

This large infrared clump so visible in Fig. 12 is not the same as the Lynga 9 clump that appears in Fig. 11; the Lynga 9 clump stars are all right at the top of the extension to the IR clump near $K=10$, represented by + signs in Figure 12. Furthermore, the IR feature is distributed far more widely than the cluster region to at least a degree away in each direction from the Lynga 9 position.

A possible explanation for Lynga 9 is that in this direction, near the galactic plane, looking toward the galactic center, the star density increases rapidly with distance. So

the apparent "main sequence" consists of stars roughly at the far distance along the line of sight. At some distance along this line of sight, there may be a dense cloud, or possibly an entire spiral arm, obscuring the view beyond. The "clump" stars of Figure 11 (as well as the much larger group of stars that show up in the 2MASS data), may consist of early-type stars behind, or more likely embedded in, this extended cloud region. What appears to be a cluster could be just a small window where the obscuration is somewhat lower so that some of the brighter stars in the cloud become visible. In all three of the Lynga 9 diagrams, including the offset field, there is a sequence parallel to the apparent main sequence - the colors of this sequence are consistent with being stars of the same type as the "clump," but just more heavily reddened.

3.8 King 25

This cluster was detected by King (1966), who suggests it has a diameter of 5 arcmin, and is moderately populated (see Fig. 8). There is no suggestion of a cluster on the 2MASS images. Its CMDs are shown in Fig. 11, together with a comparison field (upper right panel) taken 10 arcmin apart from the cluster center (see Sect. 2). Although the King 25 comparison field CMD appears different from that of the cluster field, the cluster CMD strongly resembles those of several of the other clusters in this sample. The broad "main sequence" is likely to be entirely, or primarily the rich milky way background. There probably is no cluster.

4 DISCUSSIONS AND CONCLUSIONS

The derived parameters of the program clusters are listed in Table 4. Together with reddening, distance, age and the corresponding uncertainties, we list the Galactocentric distance, derived by assuming $R_{\odot} = 8.5 kpc$ and the Galactocentric rectangular coordinates X_{\odot} , Y_{\odot} and Z_{\odot} . The adopted reference system is centered on the Sun, with the X and Y axes lying on the Galactic plane and Z perpendicular to the plane. X points in the direction of the Galactic rotation, being positive in the first and second Galactic quadrants; Y points toward the Galactic anticenter, being positive in the second and third quadrant; finally, Z is positive towards the north Galactic pole (Lynga 1982).

AL 1 and NGC 5764 are located much further from the plane than the thin disk mean scale-height; this is particularly interesting for NGC 5764, whose age is unexpected for a cluster located 300 pc above the plane. AL 1 is a very interesting object, of intermediate age, in the fourth quadrant, but very far from the galactic center and from the galactic plane.

Berkeley 80 see (Fig. 7) and NGC 5764 (see Fig 3) have elongated shapes which might indicate they are undergoing strong tidal interaction with Milky Way;

This work highlights the difficulties of working with open clusters towards the inner regions of the galaxy. The star densities are large, and increasing rapidly with distance. That causes the appearance of a main sequence on all of the CMDs in this paper, resulting simply from the geometry of the situation. Furthermore, patchy obscuration is likely

Table 4. Parameters of the studied clusters. The coordinate system is such that the Y axis connects the Sun to the Galactic Center, while the X axis is positive in the direction of galactic rotation. Y is positive toward the Galactic anti-center, and X is positive in the first and second Galactic quadrants (Lynga 1982).

<i>Name</i>	<i>E(B − V)</i>	<i>(m − M)</i>	<i>d</i> _⊙	<i>X</i> _⊙	<i>Y</i> _⊙	<i>Z</i> _⊙	<i>R</i> _G	<i>Age</i>
	mag	mag	kpc	kpc	kpc	pc	kpc	Myr
AL 1	0.34±0.05	17.2±0.2	16.9	-13.8	-9.8	-950	13.9	800±200
NGC 5764	1.00±0.05	15.3±0.2	2.8	-1.7	-2.2	290	7.1	200±100
Berkeley 80	1.10±0.05	14.8±0.2	3.3	1.7	-2.8	-70	7.3	300±100
Czernik 37	Possible cluster							
BH 150	No cluster							
BH 261	No cluster							
Lynga 9	Spiral arm?							
King 25	No cluster							

to play a role in creating apparent “clusters” that are not physical associated groups of stars.

Nevertheless, in recent work (Carraro et al 2005a,b,c) we have discovered a considerable number of neglected intermediate-age open clusters, which are going to significantly modify the open cluster age distribution and probably the typical open cluster lifetime as presently known.

ACKNOWLEDGEMENTS

The observations presented in this paper have been carried out at Cerro Tololo Interamerican Observatory CTIO (Chile). CTIO is operated by the Association of Universities for Research in Astronomy, Inc. (AURA), under a cooperative agreement with the National Science Foundation as part of the National Optical Astronomy Observatory (NOAO). The work of G. Carraro is supported by *Fundación Andes*. This study made use of Simbad and WEBDA databases. This publication makes use of data products from the 2-Micron All Sky Survey, which is a joint project of the University of Massachusetts and the Infrared Processing and Analysis Center/California Institute of Technology, funded by the National Aeronautics and Space Administration and the National Science Foundation.

REFERENCES

- Andrews A.D., Lindsay E.M. 1967, *Irish Astron. Journal* 8, 126
Baume G., Vazquez R.A., Carraro G., 2005, *MNRAS* 335, 475
van den Bergh S., Hagen G.L. 1975, *AJ* 80, 11
Bonatto, C., Bica, E., Pavani, D. B. 2004, *A&A* 427, 485
Carraro G., Girardi L., Marigo P., 2002, *MNRAS* 332, 705
Carraro G., Geisler D., Baume G., Vazquez R.A., Moitinho A., 2005a, *MNRAS* 360, 655
Carraro G., Mendez R.A., Costa E., 2005b, *MNRAS* 356, 647
Carraro G., Baume G., Vazquez R.A., Moitinho A., Geisler D., 2005c, *MNRAS*, in press ([astro-ph/0506694](#))
Czernik M. 1966, *Acta Astron.* 16, 93
Dias W.S., Alessi B.S., Moitinho A., Lepine J.R.D., 2002, *A&AS* 141, 371
Girardi L., Bressan A., Bertelli G., Chiosi C., 2000, *A&AS* 141, 371
Hasegawa T., et al., 2004, *PASJ* 56, 295
Kaluzny J., 1994, *A&AS* 108, 151
Kassisi M., Janes K.A., Friel E.D., Phelps R.L., 1997, *AJ* 113, 1723

- King I., 1966, *PASP* 78, 81
Landolt A.U., 1992, *AJ* 104, 340
Lynga G., 1964, *Lund Medd. Astron. Obs. Ser. II*, 140, 1
Lynga G., 1982, *A&A* 109, 213
Patat F., Carraro G., 2001, *MNRAS* 325, 1591
Phelps, R.L., Janes, K.A., Montgomery, K. A., 1994, *AJ* 107, 1079
Schmidt-Kaler, Th. 1982, *Landolt-Börnstein, Numerical data and Functional Relationships in Science and Technology, New Series, Group VI, Vol. 2(b)*, K. Schaifers and H.H. Voigt Eds., Springer Verlag, Berlin, p.14
Setteducati A.E., Weaver M.F., 1960, in *Newly found stellar clusters*, Radio Observatory Lab., Berkeley
Stetson P.B., 1987, *PASP* 99, 191
Wielen R., 1971, *A&A* 13, 309